

# TetriServe: Efficient DiT Serving for Heterogeneous Image Generation

Runyu Lu\*  
University of Michigan  
runyulu@umich.edu

Shiqi He\*  
University of Michigan  
shiqihe@umich.edu

Wenxuan Tan  
University of Wisconsin-Madison  
wtan45@wisc.edu

Shenggui Li  
Nanyang Technological University  
shenggui001@e.ntu.edu.sg

Ruofan Wu  
University of Michigan  
ruofanw@umich.edu

Jeff J. Ma  
University of Michigan  
jeffjma@umich.edu

Ang Chen  
University of Michigan  
chenang@umich.edu

Mosharaf Chowdhury  
University of Michigan  
mosharaf@umich.edu

## Abstract

Diffusion Transformer (DiT) models excel at generating high-quality images through iterative denoising steps, but serving them under strict Service Level Objectives (SLOs) is challenging due to their high computational cost, particularly at large resolutions. Existing serving systems use fixed degree sequence parallelism, which is inefficient for heterogeneous workloads with mixed resolutions and deadlines, leading to poor GPU utilization and low SLO attainment.

In this paper, we propose step-level sequence parallelism to dynamically adjust the parallel degree of individual requests according to their deadlines. We present TetriServe, a DiT serving system that implements this strategy for highly efficient image generation. Specifically, TetriServe introduces a novel round-based scheduling mechanism that improves SLO attainment: (1) discretizing time into fixed rounds to make deadline-aware scheduling tractable, (2) adapting parallelism at the step level and minimize GPU hour consumption, and (3) jointly packing requests to minimize late completions. Extensive evaluation on state-of-the-art DiT models shows that TetriServe achieves up to 32% higher SLO attainment compared to existing solutions without degrading image quality.

## 1 Introduction

Diffusion models [4, 5, 12, 17, 26, 28, 29] have significantly advanced text-to-image and text-to-video generation, enabling photorealistic content from natural language descriptions. They now power a wide range of commercial and creative services such as OpenAI Sora [6] and Adobe Firefly [2]. At the core of these breakthroughs are *Diffusion Transformers (DiTs)* [26], which have become the backbone of leading models including Stable Diffusion 3 (SD3) [4] and FLUX.1-dev [17]. By replacing conventional UNet architectures [12, 27], DiTs achieve higher fidelity by iteratively refining a full image

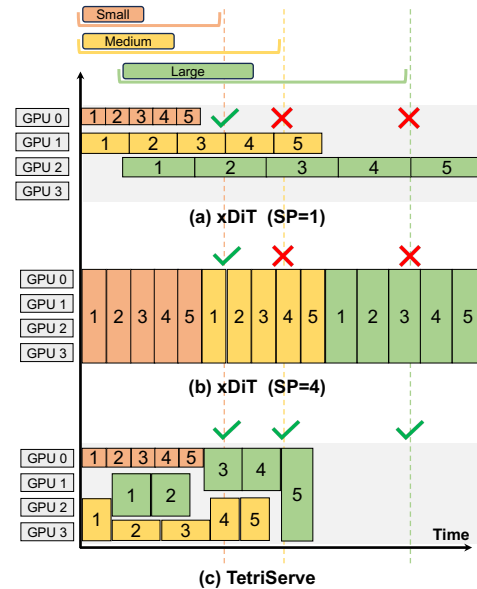


**Figure 1.** Three DiT serving requests—each with 5 denoising steps—arrive over time with different SLOs and output resolutions. DiT serving solutions using static parallelism cannot adapt and fail to meet multiple SLOs. TetriServe meets more SLOs via SLO-aware scheduling and packing.

latent representation over a sequence of discrete denoising steps, setting a new standard for generation quality.

As DiT models move into production, *online DiT serving* becomes a key systems challenge. Deployments such as Flux AI [11] must satisfy strict service level objectives (SLOs) in the form of a *deadline* for each request while sharing a fixed GPU pool across many users to minimize cost. Serving is particularly challenging because requests arrive with heterogeneous output resolutions and tight deadlines.

Despite advances in LLM serving [8, 16, 20–22, 25, 33, 37], these solutions are insufficient: DiTs have fundamentally different serving characteristics. Specifically, DiT inference differs from LLMs in three ways: (i) it is stateless, requiring

\*Both authors contributed equally to this research.

no KV cache; (ii) it is compute-bound, as multiple denoising steps operate on the full set of latent image tokens; and (iii) model sizes are small enough to fit on a single GPU. Consequently, generating a high-resolution 2048×2048 image on a single H100 GPU can take up to a minute, while a 4096×4096 image may exceed ten minutes. To meet the stringent latency demands of online serving, parallelism is essential.

The most common approach for parallelizing DiTs is *sequence parallelism (SP)* [14, 19], which partitions the sequence of image tokens across GPUs. However, simply applying a fixed degree of SP to all requests is inefficient and leads to poor SLO attainment. This is because the optimal parallel degree is highly sensitive to the input image resolution; a configuration that is ideal for one resolution can be detrimental to another. As shown in the toy example in Figure 1, fixed-degree SP approach creates a fundamental tradeoff: low parallel degrees (e.g., SP=1 or 2) are efficient for small inputs but underutilize GPUs for large ones, while high parallel degrees (e.g., SP=4 or 8) accelerate large inputs but introduce excessive communication overhead for small ones, leading to head-of-line blocking. Compounding this issue, DiT inference is non-preemptive: once a request begins execution with a fixed parallel degree, it holds its allocated GPU(s) until completion, preventing more optimal scheduling of other requests in the queue.

We observe that *step-level scheduling*, in which the degree of parallelism is adjusted across steps within each request based on its resolution and deadline, can significantly improve serving efficiency of mixed DiT workloads. High-resolution or urgent requests can be accelerated with more GPUs, while smaller or less urgent ones conserve resources. Unfortunately, we prove that finding a globally optimal step-level schedule that maximizes deadline satisfaction under a fixed GPU budget is NP-hard (§4.1). In addition, the online arrival of requests and the need for millisecond-level scheduling decisions make exhaustive optimization infeasible.

We present *TetriServe*, a step-level DiT serving system designed to maximize SLO attainment under deadline constraints. At its core, TetriServe introduces a *deadline-aware round-based scheduler* that transforms the continuous-time in the serving problem into a sequence of tractable, fixed duration rounds. In each round, the scheduler decides which requests to serve and at what GPU parallelism degree. To make these decisions, TetriServe leverages a cost model that profiles per-step latency as a function of GPU count and identifies the *minimal feasible GPU allocation* for each request that can still meet its deadline. This allows TetriServe to construct a set of candidate allocations and perform request packing with the explicit goal of minimizing the number of requests that would otherwise become late in the next round.

TetriServe further enhances GPU efficiency while preserving request deadlines. It uses *selective continuous batching* to merge steps across small-resolution requests, reducing

kernel launch overhead and boosting throughput. Meanwhile, *GPU placement preservation* and *work-conserving elastic scale-up* ensure idle GPUs are utilized without remapping distributed jobs. Together with the round-based scheduler, these techniques allow TetriServe to handle diverse DiT workloads—from small to large resolutions—while substantially improving deadline satisfaction over fixed-degree baselines.

We evaluate TetriServe on popular open source DiT models (FLUX.1-dev and SD3) and different hardware platforms (8×H100 and 4×A40 nodes). We show that TetriServe consistently outperforms xDiT [10]—a DiT-serving engine that allows different fixed SP configurations—across diverse experimental settings by up to 32% in terms of SLO attainment ratio. TetriServe is also robust to bursty request arrival patterns, diverse workload mixes, and different model-hardware combinations.

We summarize the contributions as follows:

- We cast DiT serving as a step-level GPU scheduling problem and prove its NP-hardness. Following this, we present TetriServe and introduce a deadline-aware round-based scheduler that minimizes late completions via a dynamic programming planner.
- We implement TetriServe and show substantial gains in goodput and SLO attainment over fixed-degree baselines on state-of-the-art DiT models and modern GPUs, while maintaining image quality.

## 2 Motivation

Serving DiT models has become a popular workload for modern image generation systems [3, 10]. DiT inference is both compute-intensive and latency-sensitive. To better understand the challenges of serving such workloads, in this section, we discuss DiT background, workload characteristics, and the resulting opportunities and challenges.

### 2.1 DiT Background

Diffusion models [6, 12, 26, 28, 29] have significantly advanced the quality of text-to-image and text-to-video generation, enabling the creation of photorealistic content from natural language descriptions. Each step operates on the full latent representation, removing noise based on a learned denoising function. Although early diffusion models were based on *UNet* [12, 27], modern high-quality image generators all use *Diffusion Transformers (DiT)* [7, 26] as their backbones instead of UNets. DiTs use attention [31] to capture global context and long-range dependencies.

**DiT vs LLM Parallelism.** Although both DiTs and LLMs are built upon the Transformer architecture, their inference characteristics diverge significantly, requiring different parallelism strategies. Traditional model-sharding strategies for LLMs, such as tensor and pipeline parallelism, are inefficient for DiTs. This is because DiT models are typically small

**Table 1.** Characteristics of representative input sizes for the FLUX.1-dev model [17], including latent tokens and computational cost (TFLOPs). Execution stability (CV) is measured over 20 steps on an H100 GPU for different sequence parallelism (SP) degrees.

Image Size	Tokens	TFLOPs	SP=1	SP=2	SP=4	SP=8
256 × 256	256	556.48	0.13%	0.31%	0.67%	0.62%
512 × 512	1024	1388.24	0.06%	0.15%	0.14%	0.53%
1024 × 1024	4096	5045.92	0.07%	0.12%	0.04%	0.09%
2048 × 2048	16384	24964.72	0.05%	0.11%	0.14%	0.28%

enough to fit on a single GPU. For example, the largest open-source text-to-image DiT has only 12B parameters [17] and fits comfortably on a single 80GB H100 GPU. Consequently, applying model-sharding introduces unnecessary communication overhead without the benefit of accommodating a larger model, resulting in poor hardware utilization.

DiTs adopt *sequence parallelism (SP)* [14, 18, 19], a more efficient parallel approach tailored to their compute-bound nature. In SP, token sequences (image tokens) are distributed across GPUs, enabling collaborative computation within each transformer layer. Two representative implementations are *Ulysses attention* [14], which uses all-to-all collectives to transpose tokens and heads across GPUs before local attention, and *Ring attention* [19], which arranges GPUs in a ring and passes partial Q, K, V slices peer-to-peer, overlapping communication with computation. In practice, Ulysses attention is often preferred on systems with high-bandwidth interconnects like NVLink, as its use of collective primitives can be more efficient [10].

## 2.2 Characteristics of DiT Workloads

DiT serving exhibits distinctive workload properties that affect the design of scheduling and resource management.

**Heterogeneous Inputs.** Unlike LLM workloads, where input text can vary widely in length, DiT serving workloads are characterized by a small, discrete set of possible input image resolutions [11, 30]. In this work, we focus on four representative resolutions common in production environments; their characteristics for the FLUX.1-dev model [17] are detailed in Table 1. Despite the small number of distinct input sizes, the substantial differences in their computational demands still lead to highly heterogeneous resource requirements across requests.

**Predictable Execution.** Despite input diversity, DiT inference remains compute-bound and therefore exhibits stable per-step runtimes across a wide range of input resolutions. As shown in Table 1, execution time is highly stable: profiling over 100 runs with varying sequence-parallel degrees yields a coefficient of variation (CV) below 0.7% in all cases. This low variability indicates that DiT model inference is predictable across resolutions and parallel degrees, enabling

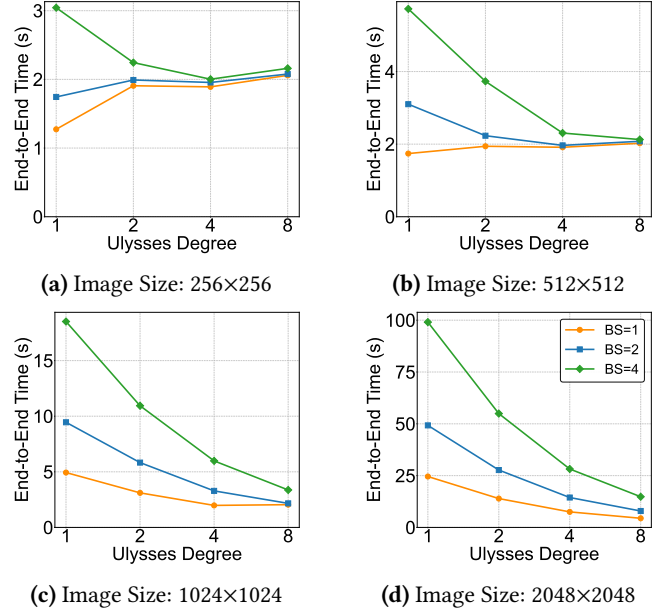


**Figure 2.** End-to-end scaling efficiency of FLUX.1-dev [17] for four resolutions on an 8xH100 server for different batch size (BS). Efficiency scales sublinearly. Larger resolutions benefit more from increased parallelism, while smaller resolutions exhibit limited scalability. Note different Y-axis scales.

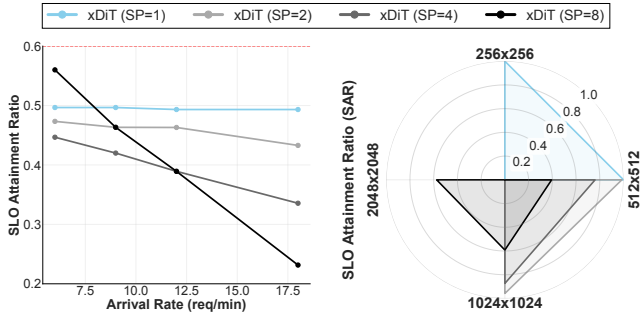
accurate performance modeling and effective deadline-aware scheduling.

**Insight 1:** DiT workloads consist of heterogeneous input requests with different output resolutions, but the per-step runtime for each resolution is highly predictable.

**Scaling Efficiency of Sequence Parallelism.** Sequence parallelism provides a mechanism to distribute tokens across GPUs, but efficiency grows sublinearly with GPU count. Two effects drive this: (i) communication overhead from collectives (all-to-all or ring exchanges) that scales with parallel degree and sequence length; and (ii) reduced per-GPU kernel efficiency when workloads are split, lowering occupancy and cache locality. Figure 2 shows that small inputs (e.g.,  $256 \times 256$ ,  $512 \times 512$ ) underutilize GPUs and scale poorly, while larger inputs (e.g.,  $1024 \times 1024$ ,  $2048 \times 2048$ ) improve efficiency though computation remains the bottleneck. This explains why in Figure 1, latency does not scale linearly with the number of GPUs.

**Insight 2:** Sequence parallelism used by DiT workloads scales sublinearly with the degree of parallelism and differently for each input resolution.

## 2.3 Opportunities and Challenges



(a) Fixed Degree Performance (b) Breakdown by Resolution

**Figure 3.** Performance of fixed degree xDiT variants under the Uniform workload. (a) The overall SLO Attainment Ratio (SAR) is low for all fixed strategies. (b) The spider plot, shown for a representative arrival rate of 12 req/min, reveals the underlying reason: low SP degrees fail on large resolutions, while high SP degrees perform poorly on small ones.

**Limitations of Current Solutions.** Conventional serving strategies using a fixed degree of parallelism are ill-suited for the heterogeneous nature of DiT workloads, a limitation illustrated in the toy example in Figure 1. With data parallelism (xDiT, SP=1), the small request meets its deadline, but the larger requests fail due to insufficient processing speed. Conversely, a high fixed parallel degree (xDiT, SP=4) handles the large request well, but it still misses the deadline (along with the medium one) due to head-of-line blocking and inefficient resource use of the small request.

This fundamental trade-off is confirmed with experimental results. As shown in Figure 3a, under a Uniform workload with a tight SLO Scale of 1.0 $\times$ , no single fixed-parallelism strategy achieves an SLO Attainment Ratio (SAR) above 0.6. The reason for this poor performance is detailed in the spider plot in Figure 3b. Different fixed strategies are only effective for specific resolutions; for example, SP=1 and SP=2 achieve a near-perfect SLO Attainment Ratio (SAR) for 256 $\times$ 256 images but fail completely for 2048 $\times$ 2048 images. Conversely, SP=4 and SP=8 can handle 2048 $\times$ 2048 images effectively but perform poorly on smaller resolutions due to scaling inefficiency and head-of-line blocking. This mismatch demonstrates that a single parallelism degree is fundamentally inefficient.

**Optimization Opportunities.** The limitations of fixed parallelism highlight a key opportunity: moving to dynamic, *step-level sequence parallelism*. As shown in Figure 1(c), our approach, TetriServe, meets all three deadlines by adapting the parallel degree for each request at the step level. It assigns fewer GPUs to the initial steps of the medium request, freeing up resources, and then scales up to meet the deadline, thus avoiding the rigid trade-offs of fixed strategies.

This flexibility to adjust the sequence parallelism degree *per step* allows a scheduler to allocate more GPUs when deadlines are tight and fewer when they are not, freeing capacity for other requests. By exploiting DiTs’ predictable

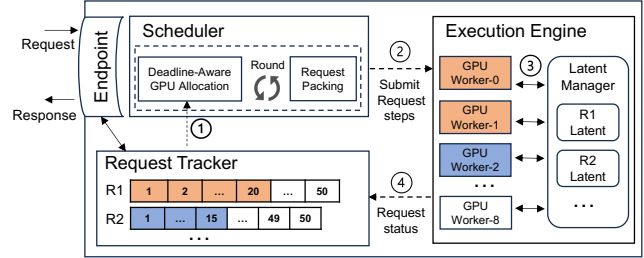


Figure 4. System overview of TetriServe.

step execution times and heterogeneous scaling behavior, this approach enables finer-grained resource shaping and better SLO attainment than conventional fixed-SP policies.

**Insight 3:** Step-level parallelism adapts GPU allocation to request deadlines, avoiding the resource waste of fixed parallelism and improving SLO satisfaction.

### 3 TetriServe Overview

TetriServe allows more DiT serving requests with heterogeneous output resolutions to meet their SLOs by judiciously scheduling and packing them on shared GPU resources. In this section, we provide an overview of how TetriServe fits in the DiT serving lifecycle to help the reader follow the subsequent sections.

**System Components.** TetriServe is designed around a scheduler that makes deadline-aware GPU allocation decisions in round-based manner. Its key components are:

- **Request Tracker:** Maintains metadata on active requests, including resolutions, deadlines, and execution states (e.g., remaining steps).
- **Scheduler:** The core component consists of *deadline-aware GPU allocation* and *round-based request packing*. At every round, it minimizes individual requests GPU consumption while maximizing SLO attainment.
- **Execution Engine:** A distributed pool of GPU workers that execute assigned diffusion steps in parallel.
- **Latent Manager:** Handles intermediate latent representations across steps, reducing redundant computation and memory overhead.

Together, these components enable TetriServe to adapt resource allocation at millisecond scale, sustaining high throughput and SLO attainment for heterogeneous DiT workloads.

**Request Lifecycle.** When a request arrives, the *Request Tracker* records its resolution, state, and deadline. The *Scheduler* then places it into the next scheduling round ①, where deadline-aware policy determines GPU allocations in terms of step numbers for each request for one round. For example, in Figure 4, it selects Request 1 for running 20 steps on 2 GPUs (orange) and Request 2 for running 15 steps on 1 GPU

(blue) for the scheduling round. Different requests are dispatched to GPU workers in the *Execution Engine* ②, which compute diffusion steps and produce intermediate latents managed by the *Latent Manager* ③. Upon completion, workers notify the request tracker to update dependent steps ④. After all steps finish, the final output is returned to the user through the endpoint.

#### 4 Deadline-Aware Round-Based Scheduler

TetriServe introduces deadline-aware scheduler designed to optimize SLO attainment for DiT serving. We begin with a formal definition of the GPU scheduling problem in the offline scenario and prove that it is NP-hard. We then propose a *round-based scheduling mechanism*, which maximizes goodput via minimizing GPU-hour consumption for each request. Later we propose enhancements so that TetriServe balances utilization, latency, and scalability in DiT serving.

##### 4.1 Problem Statement

Given a collection GPUs and requests, the DiT serving objective for each invocation of the scheduler is the following: *Find a step-level schedule that maximizes the number of requests meeting their deadlines given a fixed number of GPUs.*

**Problem Formulation.** Consider an  $N$ -GPU cluster and  $R$  outstanding requests. Each request  $req_i$  consists of a sequence of  $S_i$  dependent diffusion steps  $\{s_{i1}, s_{i2}, \dots, s_{iS_i}\}$ . Each step  $s_{ij}$  can be executed using  $k \in \{1, 2, 4, \dots, N\}$  GPUs, where  $k$  is a power of two. The execution time of a step, denoted  $T_{ij}(k)$ , is a function of  $k$ . The completion time of a request is defined as:

$$C_i = \sum_{j=1}^{S_i} [Q_{ij} + T_{ij}(A_{ij})],$$

where  $Q_{ij}$  is the queuing delay before step  $s_{ij}$  begins and  $A_{ij}$  is the number of GPUs allocated. Then we can formulate the DiT serving objective as:

$$\text{Maximize } \sum_{i=1}^R I_i, \quad \text{where } I_i = \begin{cases} 1 & \text{if } C_i \leq D_i, \\ 0 & \text{otherwise.} \end{cases}$$

This formulation is subject to the following conditions:

1. **Step Dependency:** A step  $s_{ij}$  can start only after the previous step completes:

$$\text{Start}(s_{ij}) \geq \text{Completion}(s_{i(j-1)}). \quad \forall i, \forall j > 1$$

Therefore, at most one step of a request can be executed at any time.

2. **GPU Capacity:** At any time, the total number of GPUs allocated across all steps cannot exceed  $N$ :

$$\sum_{i=1}^R \sum_{j=1}^{S_i} A_{ij}(t) \leq N, \quad \forall t$$

**Table 2.** Notations used in the GPU Scheduling Problem.

Symbol	Description
$N$	Total number of GPUs.
$R$	Number of requests.
$S_i$	Number of steps in request $req_i$ .
$D_i$	Deadline of request $req_i$ .
$T_{ij}(k)$	Execution time of step $s_{ij}$ with $k$ GPUs.
$Q_{ij}$	Queueing delay before step $s_{ij}$ starts.
$A_{ij}$	GPU allocation for step $s_{ij}$ .
$C_i$	Completion time of request $req_i$ .

where  $A_{ij}(t)$  denotes the GPUs allocated to step  $s_{ij}$  if it is running at time  $t$ , and zero otherwise.

The goal is to find a set of GPU assignments  $\{A_{ij}\}$  that maximizes the number of requests meeting their deadlines.

**NP-hardness.** To highlight the computational complexity, we consider the special case where each request has a single non-preemptive step ( $S_i = 1$ ). Time is discretized into slots  $\mathcal{T} = \{0, 1, \dots, T_{\max} - 1\}$ . Let  $\mathcal{K} = \{1, 2, 4, \dots, N\}$  denote the allowed GPU allocations. For each request  $i$ , start time  $t \in \mathcal{T}$ , and GPU count  $k \in \mathcal{K}$ , introduce a binary decision variable:

$$x_{i,t,k} = \begin{cases} 1 & \text{if request } i \text{ starts at time } t \text{ with } k \text{ GPUs,} \\ 0 & \text{otherwise.} \end{cases}$$

**Objective.** Maximize the number of requests completing by their deadlines:

$$\max \sum_i \sum_{t \in \mathcal{T}} \sum_{k \in \mathcal{K}} x_{i,t,k}.$$

**Constraints.**

$$\sum_{t \in \mathcal{T}} \sum_{k \in \mathcal{K}} x_{i,t,k} \leq 1, \quad \forall i, \quad (1)$$

$$\text{arrival\_time}(i) \leq t, \quad \forall i, \quad (2)$$

$$t + T_i(k) \leq D_i, \quad \forall i, t, k, \quad (3)$$

$$\sum_i \sum_{k \in \mathcal{K}} \sum_{u \in [t, t+T_i(k)-1]} k \cdot x_{i,t,k} \leq N, \quad \forall t, u \in \mathcal{T}, \quad (4)$$

$$x_{i,t,k} \in \{0, 1\}, \quad \forall i, t, k. \quad (5)$$

Constraint (1) ensures each request starts at most once. Constraints (2) and (3) enforce arrival times and deadline feasibility. Constraint (4) enforces that at any time slot  $u$ , the sum of GPUs assigned to running requests does not exceed system capacity  $N$ . Constraint (5) enforces integrality.

This Zero-one Integer Linear Program (ZILP) exactly captures the offline DiT serving problem in the single-step case, where  $I_i = \sum_{t \in \mathcal{T}} \sum_{k \in \mathcal{K}} x_{i,t,k}$ . Since solving such formulations is NP-hard [15, 24, 35], **multi-step DiT serving is NP-hard** as well.

## 4.2 Round-Based Scheduling

Step-level scheduling for DiT serving is NP-hard, making global optimization expensive. To enable practical scheduling, TetriServe adopts a round-based heuristic: instead of scheduling steps arbitrarily in a continuous global timeline, we discretize execution into rounds, where each round corresponds to a fixed-length GPU execution window. This allows us to (i) limit the scheduling search space and (ii) enable efficient preemption between rounds. Within each round, TetriServe determines the minimal required GPU allocation for requests and dynamically packs these requests to maximize SLO attainment ratio.

**4.2.1 Deadline-Aware GPU Allocation.** Exhaustively enumerating GPU allocations for each step is infeasible, and over-allocation wastes resources due to scaling inefficiencies in DiT models (e.g., kernel launch and communication overheads). While more GPUs reduce latency, they increase total GPU hours. To balance these trade-offs, TetriServe identifies the minimal GPU allocation needed for each request to meet its deadline at the beginning of each round. Since required allocation depends mainly on resolution and deadline, this approach avoids exploring the full allocation space.

For a step  $s_{ij}$ , the execution time  $T_{ij}(k)$  is a function of the number of GPUs  $k$ . The GPU hour for executing step  $s_{ij}$  with  $k$  GPUs is  $k \times T_{ij}(k)$ . The goal is to minimize the total GPU hour for each request:

$$\min_{\{A_{ij}\}} \sum_{j=1}^{S_i} (A_{ij} \times T_{ij}(A_{ij})) \quad \text{s.t.} \quad \sum_{j=1}^{S_i} (Q_{ij} + T_{ij}(A_{ij})) \leq D_i$$

where  $A_{ij}$  is the GPU allocation for step  $s_{ij}$ .

**Offline Profiling for Cost Model.** To make the optimization tractable, TetriServe profiles execution times offline. For every step type  $s_{ij}$  and GPU count  $k \in \{1, 2, 4, \dots, N\}$ , we measure the actual execution time  $T_{ij}(k)$ . From this, we derive the GPU hour  $k \times T_{ij}(k)$  and store it in a lookup table. At runtime, TetriServe simply enumerates candidate GPU assignments using these pre-profiled values.

The above process aims to assign each request the minimum number of GPUs required to meet its deadline while minimizing the total GPU hours. Figure 5 illustrates this process with a concrete example: three requests (R1–R3), each with five steps, arrive over time. R1 has a small resolution (e.g., 256) and is fixed at SP=1 since higher parallelism would reduce efficiency (see Fig. 2). For R2 and R3, TetriServe identifies GPU allocations with two parallelism degrees that just meet their deadlines while minimizing overall GPU usage. The GPU allocations produced by this selection serve as the input to the subsequent request packing stage, where TetriServe schedules requests across GPUs to maximize goodput.

**4.2.2 Request Packing.** The objective of scheduling is to maximize the number of requests that complete before

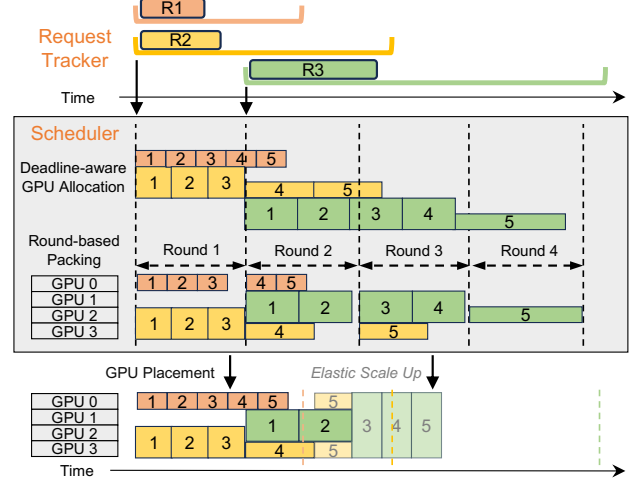


**Figure 5.** Illustration of TetriServe’s scheduling process. The progression is shown from top to bottom: each row represents an intermediate scheduling step, while the final row shows the actual GPU allocation decision. Time is fixed across rows.

their deadlines. To make the problem tractable, we approximate it by minimizing the number of requests that become *definitely late*—those that cannot meet their deadlines even under maximal parallelism if not advanced in the current round. Deadline-aware GPU allocation determines the minimal GPU allocations needed for each request to meet its deadline while minimizing GPU hours. This makes it possible to pack more requests into each round and thereby reduce the number that would otherwise be definitely late.

After deadline-aware GPU allocation, each request  $req_i$  is described by a set of allocations  $(s_i^m, A_i^m)$ , where  $s_i^m$  is the number of steps executed with allocation  $A_i^m$ , and per-step times  $T_i(A_i^m)$  are obtained from the cost model. To schedule requests across  $N$  GPUs, TetriServe divides time into *rounds* of fixed duration  $\tau$ , which serves as the scheduling granularity. The choice of  $\tau$  balances overhead and responsiveness: shorter rounds allow finer-grained preemption and more adaptive scheduling, while longer rounds reduce overhead but make scheduling coarser.

At the beginning of each round  $r$  (time  $t_r$ ), the scheduler considers all pending requests and their allocations, and decides which to place within the  $N$  GPUs. Within a round of duration  $\tau$ , if GPU allocation  $m$  of request  $i$  is chosen, the number of steps that can complete is

$$q_i^m = \min \left\{ s_i^m, \left\lfloor \frac{\tau}{T_i(A_i^m)} \right\rfloor \right\}.$$

Options with  $q_i^m = 0$  are discarded to avoid wasting resources. Choosing option  $o \in \{\text{none}, 1, 2, \dots\}$  updates the remaining steps as

$$\tilde{s}_i^m(o) = s_i^m - \mathbb{1}[o = m] q_i^m,$$

**Algorithm 1:** DP Round Scheduler

---

**Input** : Pending requests  $R$  with  $\{(s_i^m, A_i^m)\}_{m \in \mathcal{M}_i}$  and  $T_i(\cdot)$ ; capacity  $N$ ; round length  $\tau$ ; current time  $t_r$

**Output**: Selected plan

```

1  $t_{r+1} \leftarrow t_r + \tau$ 
2 foreach  $i \in R$  do
3   foreach  $m \in \mathcal{M}_i$  do
4      $q_i^m \leftarrow \min\{s_i^m, \lfloor \tau/T_i(A_i^m) \rfloor\}$ 
5      $T_i^{\min} \leftarrow \min_{k \in K} T_i(k)$ 
6      $\mathcal{O}_i \leftarrow \{\text{none}\} \cup \{m \in \mathcal{M}_i \mid q_i^m > 0 \wedge A_i^m \leq N\}$ 
7     foreach  $o \in \mathcal{O}_i$  do
8       foreach  $m \in \mathcal{M}_i$  do
9          $\tilde{s}_i^m(o) \leftarrow s_i^m - \mathbb{I}[o = m] \cdot q_i^m$ 
10         $\text{LB}_i(o) \leftarrow (\sum_{m \in \mathcal{M}_i} \tilde{s}_i^m(o)) T_i^{\min}$ 
11         $\text{sv}_i(o) \leftarrow \mathbb{I}[t_{r+1} + \text{LB}_i(o) \leq D_i]$ 
12         $w_i(o) \leftarrow 0$  if  $o = \text{none}$  else  $A_i^o$ 
13 Initialize  $\text{dp}[0..N] \leftarrow -\infty$ ,  $\text{dp}[0] \leftarrow 0$ 
14 foreach  $i \in R$  do
15    $\text{next}[0..N] \leftarrow \text{dp}$ 
16   for  $c = 0$  to  $N$  do
17     foreach  $o \in \mathcal{O}_i$  do
18       if  $w_i(o) \leq c$  then
19          $\text{next}[c] \leftarrow \max\{\text{next}[c], \text{dp}[c - w_i(o)] + \text{sv}_i(o)\}$ 
20    $\text{dp} \leftarrow \text{next}$ 
21  $c^* \leftarrow \arg \max_c \text{dp}[c]$ 
22 return plan reconstructed from back-pointers at  $c^*$ 

```

---

clipped at zero, where  $\mathbb{I}[o = m]$  equals 1 if  $o = m$  and 0 otherwise. The next round begins at  $t_{r+1} = t_r + \tau$ .

To decide which requests must be scheduled *now*, we identify those that would become *definitely late* at  $t_{r+1}$  if not advanced in this round. Using the fastest possible step time  $T_i^{\min} = \min_{k \in \{1, 2, 4, \dots, N\}} T_i(k)$ , we define the *residual completion time lower bound* under option  $o$  as

$$\text{LB}_i(o) = \left( \sum_m \tilde{s}_i^m(o) \right) T_i^{\min},$$

where  $\tilde{s}_i^m(o)$  is the updated step count. A request survives only if

$$t_{r+1} + \text{LB}_i(o) \leq D_i.$$

Each option  $o$  consumes  $w_i(o)$  GPUs:  $w_i(\text{none}) = 0$ ,  $w_i(m) = A_i^m$ . The per-round scheduling problem is therefore to select at most one option per request, with total GPU  $\leq N$ , maximizing the number of requests that survive to the next round. By anchoring scheduling decisions on the round duration  $\tau$ , TetriServe balances preemption overhead and responsiveness, while ensuring urgent requests receive priority.

**Dynamic Programming.** Naively enumerating all per-request options  $\mathcal{O}_i$  for feasible packings within a round is exponential in the number of requests and quickly becomes intractable. We observe that the per-round decision has the *group-knapsack* structure: for each request  $i$  (a group), we must choose at most one option  $o$  (run one of its GPU allocation this round or none), each option consumes width (GPUs) and yields a binary “survival” value indicating whether the request is *not definitely late* at the next round start. This lets us replace exhaustive search with a dynamic program (DP) that maximizes the number of surviving requests under the round capacity  $N$ .

Concretely, the DP state  $\text{dp}[c]$  stores, after processing the first  $i$  requests, the maximum number of surviving requests achievable with exactly capacity  $c \in \{0, \dots, N\}$  consumed in the current round. For request  $i$ , we build its option set  $\mathcal{O}_i$  once (group constraint): none (consume zero GPUs, no progress) and one option per allocation  $m$  that can make progress in this round, i.e.,  $q_i^m = \lfloor \tau/T_i(A_i^m) \rfloor > 0$  and  $A_i^m \leq N$ . For each option  $o \in \mathcal{O}_i$ , we compute:

1. **Line 9:** the updated remaining steps  $\tilde{s}_i^m(o)$ .
2. **Line 10:** a conservative lower bound  $\text{LB}_i(o)$  on the residual processing time from  $t_{r+1} = t_r + \tau$ .
3. **Line 12:** its width  $w_i(o)$  (0 for none,  $A_i^m$  for allocation  $m$ ).

We then set the survival indicator  $\text{sv}_i(o) = \mathbb{I}[t_{r+1} + \text{LB}_i(o) \leq D_i]$ . The DP transition iterates options once per request (respecting the group constraint) and, for each capacity  $c$ , admits only options with  $w_i(o) \leq c$  (respecting the capacity constraint):

$$\text{next}[c] \leftarrow \max\{\text{next}[c], \text{dp}[c - w_i(o)] + \text{sv}_i(o)\}.$$

Using a rolling array yields  $O(N)$  space. Since each request contributes at most  $|\mathcal{O}_i|$  options, DP runs in  $O(RN)$  time and  $O(N)$  space per round (rolling array), which is tractable even at millisecond-scale rounds for moderate  $N$ . This is orders of magnitude cheaper than enumerating all feasible packing combinations.

**Round Duration.** Algorithm 1 schedules in fixed-length rounds of duration  $\tau$ . The choice of  $\tau$  balances two factors: short rounds reduce admission delay for new requests but increase scheduling frequency, while long rounds amortize scheduling cost but risk larger queueing delay and deadline misses. For a given GPU configuration (e.g., NVIDIA H100), TetriServe adapts  $\tau$  to the step execution times of requests across different resolutions, so that requests with heterogeneous step lengths can finish around the same round boundary. This minimizes idle bubbles while keeping  $\tau$  short enough to avoid excessive queueing delay. We will further discuss the impact of round duration in the evaluation section (§6.4).

**4.2.3 Efficient GPU Placement and Allocation.** In the round-based framework (Algorithm 1), TetriServe improves efficiency via two complementary steps: *placement preservation* and *work-conserving elastic scale-up*, illustrated in Figure 5. First, to avoid idle bubbles between rounds, TetriServe adopts a placement-aware policy: requests continue on the same GPUs across consecutive rounds whenever possible. This eliminates state-transfer delays and ensures immediate progress at round boundaries.

Second, any GPUs left idle after placement are reclaimed through a work-conserving elastic scale-up policy. Requests with sufficient remaining steps are granted additional GPUs if  $T_i(k'_i) < T_i(k_i)$ , prioritizing those that benefit most from parallelism. This ensures no GPU remains unused within a round, reducing future load and improving deadline satisfaction. Together, placement preservation minimizes inter-round stalls, while elastic scale-up guarantees work conserving allocation within each round.

## 5 Implementation

TetriServe is implemented in 5033 lines of Python and C++ code. We reuse components from existing solutions, including xDiT [10], vLLM [16], MuxServe [9], SGLang [37].

**Scheduler.** The scheduler’s core decision loop is implemented in C++ and exposed via lightweight bindings, achieving millisecond-level control-plane latency.

**VAE Decoder Sequential Execution.** The VAE decoder imposes a large activation-memory footprint at high resolutions and batch sizes, whereas its wall-clock cost is very small relative to diffusion steps. Accordingly, we adopt sequential per-request decoding to bound peak memory by avoiding concurrent decoder activations across a batch. Because the decoder is largely off the critical path, this design does not increase end-to-end latency. The reduced peak usage also increases headroom for model state and communication buffers, lowering the risk of out-of-memory failures under mixed workloads.

**Communication Process Groups Warmup.** We pre-create process groups for all relevant combinations of devices (e.g.,  $\binom{8}{k}$  groups for degrees  $k \in \{1, \dots, 8\}$ ). Creating the group itself is lightweight and does not materially consume GPU memory. However, the *first* invocation on a group initializes NCCL [23] channels and allocates persistent device buffers for subsequent collectives. Proactively warming *every* group therefore inflates memory usage and can exceed available HBM. To balance startup latency and memory footprint, we warm only a compact set of commonly used, overlapping groups (e.g., [0,1,2,3], [0,2,3,4]) and defer others to on-demand warmup. Empirically, this strategy preserves performance while maintaining low peak memory.

**Latent Transfer.** Because FluidSP executes at step granularity, intermediate latents and lightweight metadata must be

handed off across GPU groups. We provide a Future-like abstraction for latents that enables asynchronous, non-blocking transfer between steps. Latent tensors are compact (in the compressed latent space), so transfer overhead is negligible; consequently, the scheduler excludes latent-transfer time from deadline accounting.

**Selective Continuous Batching.** Batching in diffusion inference is only effective for identical, small-resolution requests that would otherwise underutilize GPUs. This creates a throughput-latency trade-off. Our scheduler employs a selective, step-level batching strategy that only groups requests if their SLOs are not compromised, thus improving resource utilization without harming latency.

## 6 Evaluation

In this section, we evaluate the performance of TetriServe with state-of-the-art solutions on different Workloads. Our key findings are as follows

- TetriServe consistently outperforms fixed-SP baselines across diverse experimental settings by up to 32% (§6.2). Its benefits hold from the smallest to the largest resolution.
- TetriServe is more robust to burst request arrival patterns and can adapt to changing output resolution requests (§6.3).
- Our sensitivity analysis discusses the impact of step granularity, homogeneous workloads, arrival rate on TetriServe’s performance, and confirms that TetriServe’s performance advantage holds across different arrival rates and for homogeneous workloads, where it still outperforms the best-performing baselines (§6.4).

### 6.1 Methodology

**Testbed.** We conducted our experiments on two GPU clusters. The first cluster comprises nodes with 8 NVIDIA H100-80GB HBM3 GPUs interconnected with NVLink 4.0, providing 900 GB/s inter-GPU bandwidth. The second cluster features nodes with 4 NVIDIA A40-48GB GPUs connected in pairs using NVLink and interfaced to the host via PCIe 4.0. Our software environment is based on NVIDIA’s NGC container, which includes CUDA 12.5, NCCL 2.22.3 [23], PyTorch 2.4.0 [36], and xDiT[10] (git-hash 8f4b9d30).

**Models and Metrics.** Among open-source models, we pick *FLUX.1-dev* [17] and *Stable Diffusion 3 Medium* (SD3) [4] as representative, widely used choices. We evaluate TetriServe on these two models on H100 and A40 clusters, respectively, to demonstrate effectiveness across state-of-the-art DiT models. We report SLO Attainment Ratio (SAR; fraction of requests that finish within SLO) as our primary metric.

**Baselines.** We compare TetriServe against xDiT [10], a state-of-the-art DiT inference engine that uses parallelization.

Since xDiT does not support serving interface and scheduling logic, we implement and evaluate four fixed-parallelism strategies for xDiT: xDiT (SP=1), xDiT (SP=2), xDiT (SP=4), and xDiT (SP=8), where each request is parallelized across a fixed number of GPUs throughout its execution.

**SLO Settings.** We adopt resolution-specific latency targets grounded in user-perceived responsiveness. Prior research [1] reports that 63% of the users prefer a maximum response delay of 5 seconds in interactive settings. Accordingly, we cap the target at 1.5 seconds for small images and set an upper bound of 5.0 seconds for the largest resolution. Concretely, we set per-request baseline SLOs as follows: (256, 256) = 1.5 s, (512, 512) = 2.0 s, (1024, 1024) = 3.0 s, and (2048, 2048) = 5.0 s. We also scale SLOs using a SLO Scale and sweep it from 1.0× to 1.5× relative to each resolution’s baseline.

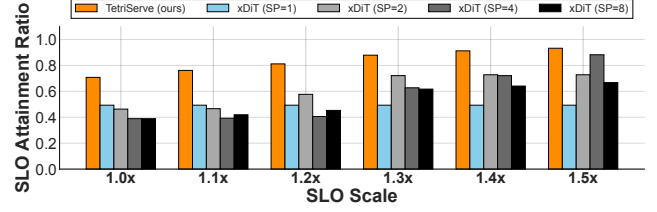
**Workload and Dataset.** We sample 300 prompts from DiffusionDB [32] to generate requests. By default, requests arrive following Poisson processes, with arrival rates of 12 request-/minute(rpm).

As for input resolutions, we consider two workload mixes: (i) *Uniform* consists of equal number of requests for input resolutions {256, 512, 1024, 2048}; and (ii) *Skewed*, which samples input resolutions according to an exponential weight over latent length,  $p_i \propto \exp(\alpha \cdot L_i/L_{\max})$ , with  $\alpha = 1.0$  and  $L_i = (H_i \cdot W_i)/16^2$ , thereby biasing the distribution toward larger resolutions.

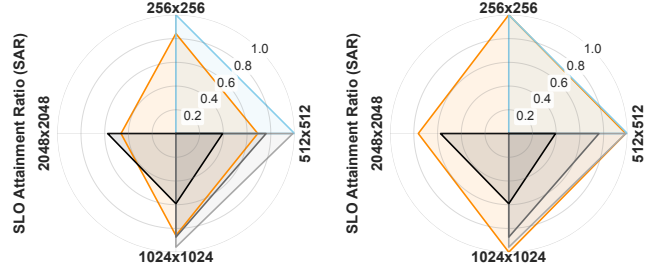
## 6.2 End-to-End Performance

**TetriServe Improves SAR.** Figures 6 and 7 show the end-to-end SLO Attainment Ratio (SAR) of TetriServe compared to fixed-parallelism baselines for FLUX on H100s for both the Uniform and Skewed workload mixes at an arrival rate of 12 requests per minute. As shown in Figures 6a and 7a, TetriServe consistently achieves the highest SAR across all SLO scales and both workload distributions. This demonstrates the effectiveness of its step-level parallelism control and request packing, which allow it to dynamically adapt to the workload and outperform the rigid strategies of the baselines.

On average, TetriServe outperforms the best fixed parallelism strategy by 10% for the Uniform mix and 15% for the Skewed mix. The performance gap is particularly pronounced at tighter SLOs. For instance, with an SLO scale of 1.1× in the Uniform mix, TetriServe outperforms the best baseline by 28%. Similarly, in the Skewed mix with a 1.2× SLO scale, TetriServe’s SAR is 32% higher than the best-performing fixed strategy. This highlights TetriServe’s superior performance under challenging, tightly constrained Workloads.



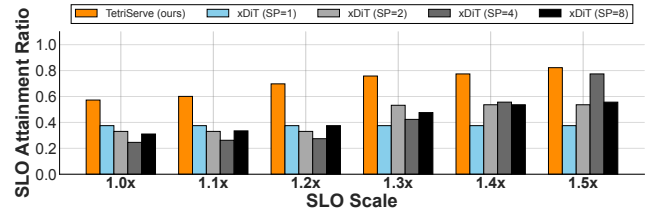
(a) SAR of Uniform Workload



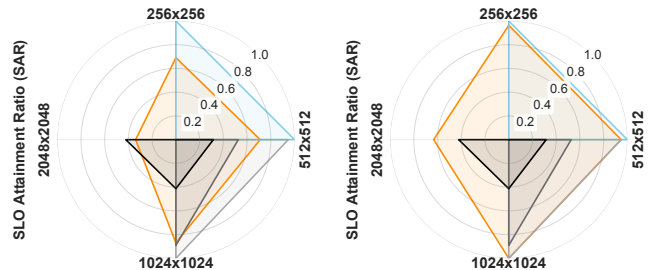
(b) Uniform, SLO Scale=1.0×

(c) Uniform, SLO Scale=1.5×

**Figure 6.** End-to-end performance on the Uniform workload at 12 req/min. **(Top)** TetriServe achieves the highest SLO Attainment Ratio (SAR) across all SLO scales. **(Bottom)** The spider plots show that xDiT variants only perform well for specific resolutions, TetriServe delivers high SAR across all resolutions no matter tight or loose SLO Setting.



(a) SAR of Skewed Workload



(b) Skewed, SLO Scale=1.0×

(c) Skewed, SLO Scale=1.5×

**Figure 7.** End-to-end performance on the Skewed workload at 12 req/min. **(Top)** TetriServe again achieves the highest SLO Attainment Ratio (SAR) across all SLO scales. **(Bottom)** The spider plots confirm that TetriServe’s adaptive parallelism provides robust performance across all resolutions, even in a workload dominated by large images

**TetriServe Benefits All Resolutions.** TetriServe’s strength lies in its ability to deliver high SAR across all request resolutions, unlike fixed strategies that only excel at specific

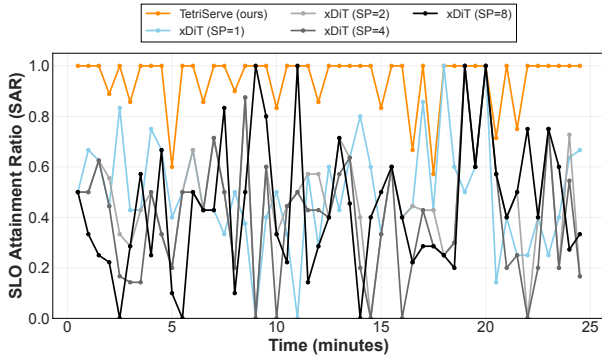


**Figure 8.** Performance stability under the Uniform workload at 12 req/min with a 1.5x SLO Scale. TetriServe maintains a high and stable SLO Attainment Ratio (SAR) over time, which handles burstiness well.

ones. The spider plots in the bottom row of Figures 6 and 7 break down SAR by resolution. With a relaxed SLO of 1.5x (Figures 6c and 7c), TetriServe achieves near-perfect SAR across all resolutions for both workload mixes, consistently outperforming all xDiT baselines. Under the tightest SLO of 1.0x (Figures 6b and 7b), TetriServe provides the best overall performance. While some fixed-parallelism strategies may marginally outperform TetriServe on a single resolution (e.g., xDiT SP=1 on 256px), they perform poorly on others. In contrast, TetriServe dynamically adapts its parallelism, providing high SAR across the entire spectrum of resolutions. It avoids over parallelization for less urgent requests and prioritizes more GPU resources for more urgent requests, thus performing well on all resolutions.

### 6.3 Performance Stability under Bursty Traffic

TetriServe maintains a high and stable SAR even under bursty arrival patterns, whereas fixed-parallelism approaches exhibit significant performance oscillations. For instance, Figure 8 plots the SAR over time for the Uniform mix (12 req/min, SLO Scale=1.5x). TetriServe’s SAR remains consistently high with low variance. In contrast, the fixed xDiT variants suffer from periodic drops in SAR, a result of utilization bubbles and subsequent queuing delays when bursty arrivals create contention.

The key to TetriServe’s stability is its ability to adapt the degree of sequence parallelism (SP) at the step level. As shown in Figure 9, when bursty arrivals create contention, TetriServe dynamically raises the SP degree for computationally intensive, urgent requests to shorten their critical path and reduce SLO violation risk. Conversely, it scales down the degree for less urgent requests steps while maintain SLO Attainment Ratio. This fine-grained, adaptive parallelism is how TetriServe handles burstiness and achieves superior efficiency and responsiveness compared to rigid, fixed-degree systems.

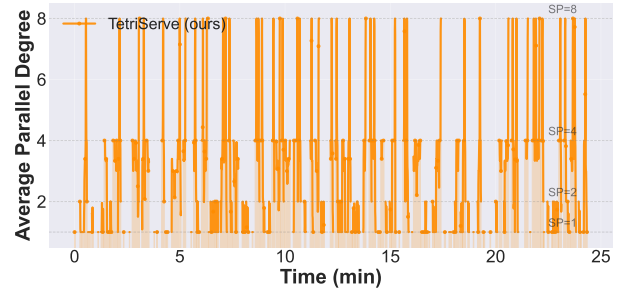
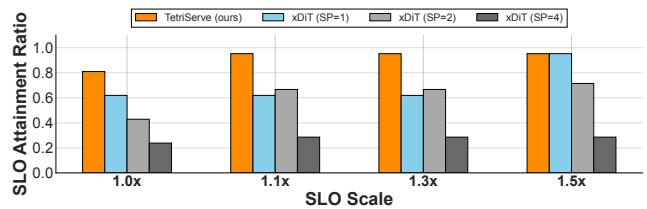
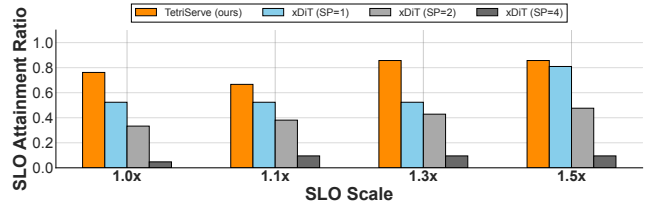


**Figure 9.** Average parallel degree of TetriServe during serving under the Uniform workload (1.5x SLO Scale). TetriServe dynamically adjusts sequence parallelism (SP) per request, assigning more GPUs to intensive requests (longer bars) to meet deadlines.



(a) SAR vs. SLO Scale (SD3, Uniform mix)



(b) SAR vs. SLO Scale (SD3, Skewed mix)

**Figure 10.** TetriServe’s performance on the Stable Diffusion 3 (SD3) model. The plots show the SLO Attainment Ratio (SAR) as a function of SLO Scale for the Uniform mix (left) and Skewed mix (right) on A40 GPUs. In both workloads, TetriServe consistently outperforms all xDiT variants

### 6.4 Sensitivity Analysis

**Different GPU Settings and Models.** On SD3, trends align with FLUX. In both the Uniform mix (Figure 10a) and Skewed mix (Figure 10b), TetriServe achieves the highest SAR across all SLO scales, with the largest margins at tight SLOs (1.0x). As SLOs loosen, fixed SP2 and SP4 improve but remain below TetriServe, while fixed SP1 underutilize and plateau. This indicates the benefits generalize to a different DiT architecture. On the A40 cluster, NVLink links GPUs only in pairs; at SP=4, collectives traverse PCIe, and even at SP=2 poor placement can cross PCIe. For SD3 this communication path becomes the bottleneck, so SP2 and SP4 perform notably worse than on H100.

**Arrival Rate.** Figure 11 shows the SAR of different scheduling strategies under the Uniform mix with a tight SLO

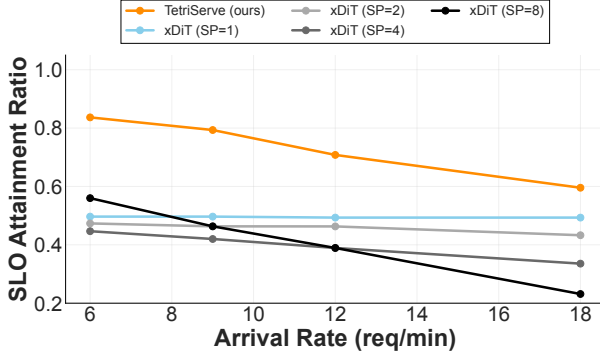


**Figure 11.** SLO Attainment Ratio vs. arrival rate under the Uniform mix (SLO Scale=1.0x). TetriServe gracefully handles increasing load, maintaining a high SAR.

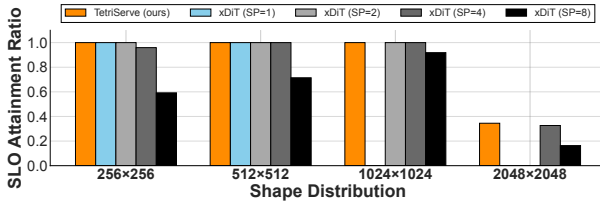


**Figure 12.** SLO Attainment Ratio for homogeneous workloads at 12 req/min with a 1.5x SLO Scale. Each group of bars represents a workload with only one resolution type. TetriServe consistently achieves the highest SAR across all resolutions.

of 1.0x as the arrival rate increases from 6 to 18 req/min. TetriServe demonstrates superior performance across the full range of arrival rates. At low-to-medium rates, TetriServe maintains a consistently high SAR, while fixed-parallelism strategies already show signs of degradation. At high arrival rates, where the system is under heavy load, TetriServe’s SAR remains relatively high, showcasing graceful degradation.

**Homogeneous Resolutions.** To isolate the effect of input resolution on parallelism strategies, we evaluate homogeneous workloads containing only a single resolution. Figure 12 shows the SLO Attainment Ratio (SAR) for workloads consisting of only one resolution type at an arrival rate of 12 req/min and an SLO Scale of 1.5x. Even in these simplified scenarios, TetriServe still achieves the highest SAR across all resolution types. This demonstrates that TetriServe’s adaptive scheduling is effective not only for mixed workloads but also for homogeneous ones, as it can still optimize resource allocation to better meet deadlines.

**Step Granularity.** We examine the impact of step granularity, which defines how frequently TetriServe can reschedule and change the parallel degree for an in-flight request. This presents a fundamental trade-off: fine-grained control (e.g., every 1-2 steps) offers maximum flexibility at the cost of high scheduling overhead, while coarse-grained control

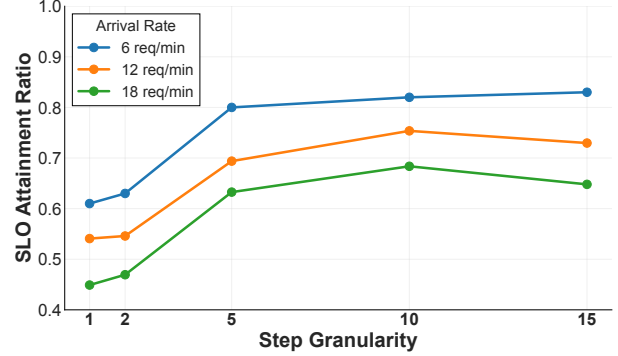


**Figure 13.** Sensitivity of SLO Attainment Ratio to step granularity and arrival rate under the Uniform mix (SLO Scale=1.0x). A moderate granularity (5/10 steps) provides the most robust performance as system load increases, balancing scheduling flexibility and overhead.

(e.g., every 10 steps) minimizes overhead but creates longer, non-preemptible execution blocks that reduce adaptability. Figure 13 illustrates this trade-off under the Uniform mix (SLO Scale=1.0x) across different arrival rates. At low rates, performance is less sensitive to granularity. However, as load increases, a moderate granularity of 5 steps proves most robust, balancing adaptability and overhead. Very fine-grained control (1 step) suffers from excessive overhead, while coarse-grained control (10 steps) is too inflexible to handle preemption, leading to lower SLO attainment.

## 7 Related Work

**LLM Serving Frameworks.** LLM serving systems [16, 37] are not directly applicable to DiT workloads. Systems like LoongServe [33] optimize for the prefill-decode stages of long-context LLMs, while PrefillOnly [8] targets memory efficiency for short, prefill-intensive jobs. Neither is suited for the multi-step, stateless inference pattern of DiTs.

**DiT Model Inference and Serving Frameworks.** DiT-specific serving systems are still emerging. xDiT [10] uses a fixed sequence parallelism strategy, which is inefficient for heterogeneous workloads. DDiT [13] is designed for video generation and only focuses on maximizing throughput, not meeting per-request deadlines. TetriServe uniquely prioritizes SLO attainment for heterogeneous requests through cost-model driven scheduling.

**Text-to-Image Caching Systems.** Caching systems can accelerate text-to-image generation. Nirvana [3] reuses intermediate latents for similar prompts, while MoDM [34] caches final images for refinement with smaller models. These approaches reduce computation and are orthogonal to scheduling. TetriServe’s scheduling is complementary and can be combined with such caching techniques.

## 8 Conclusion

We presented TetriServe, a deadline-aware round-based diffusion transformer (DiT) serving system that addresses the challenge of meeting SLO under heterogeneous workloads. TetriServe dynamically adapts parallelism at the *step level*, guided by a profiling-driven cost model and a deadline-aware scheduling algorithm. Through extensive evaluation on DiT models and hardware platforms, TetriServe consistently outperforms fixed parallelism baselines, achieving up to 32% higher SLO Attainment Ratio and delivering robust performance across various input resolutions, workload distributions, and arrival rates.

## Acknowledgments

We would like to thank the SymbioticLab and UsesysLab members for their insightful feedback.

## References

- [1] Tahir Abbas, Ujwal Gadiraju, Vassilis-Javed Khan, and Panos Markopoulos. 2022. Understanding user perceptions of response delays in crowd-powered conversational systems. *Proceedings of the ACM on Human-Computer Interaction* 6, CSCW2 (2022), 1–42.
- [2] Shubham Agarwal, Subrata Mitra, Sarthak Chakraborty, Srikrishna Karanam, Koyel Mukherjee, and Shiv Kumar Saini. 2024. Approximate Caching for Efficiently Serving Text-to-Image Diffusion Models. In *21st USENIX Symposium on Networked Systems Design and Implementation (NSDI 24)*. USENIX Association, Santa Clara, CA, 1173–1189. <https://www.usenix.org/conference/nsdi24/presentation/agarwal-shubham>
- [3] Shubham Agarwal, Subrata Mitra, Sarthak Chakraborty, Srikrishna Karanam, Koyel Mukherjee, and Shiv Kumar Saini. 2024. Approximate Caching for Efficiently Serving Text-to-Image Diffusion Models. In *21st USENIX Symposium on Networked Systems Design and Implementation (NSDI 24)*. USENIX Association, Santa Clara, CA, 1173–1189. <https://www.usenix.org/conference/nsdi24/presentation/agarwal-shubham>
- [4] Stability AI. 2024. Stable Diffusion 3 Medium. <https://huggingface.co/stabilityai/stable-diffusion-3-medium>.
- [5] Stability AI. 2024. Stable Diffusion 3.5 Large. <https://huggingface.co/stabilityai/stable-diffusion-3.5-large>.
- [6] Tim Brooks, Bill Peebles, Connor Holmes, Will DePue, Yufei Guo, Li Jing, David Schnurr, Joe Taylor, Troy Luhman, Eric Luhman, Clarence Ng, Ricky Wang, and Aditya Ramesh. 2024. Video generation models as world simulators. (2024). <https://openai.com/research/video-generation-models-as-world-simulators>
- [7] Alexey Dosovitskiy, Lucas Beyer, Alexander Kolesnikov, Dirk Weissenborn, Xiaohua Zhai, Thomas Unterthiner, Mostafa Dehghani, Matthias Minderer, Georg Heigold, Sylvain Gelly, Jakob Uszkoreit, and Neil Houlsby. 2021. An Image is Worth 16x16 Words: Transformers for Image Recognition at Scale. In *International Conference on Learning Representations (ICLR)*.
- [8] Kuntai Du, Bowen Wang, Chen Zhang, Yiming Cheng, Qing Lan, Hejian Sang, Yihua Cheng, Jiayi Yao, Xiaoxuan Liu, Yifan Qiao, Ion Stoica, and Junchen Jiang. 2025. PrefillOnly: An Inference Engine for Prefill-only Workloads in Large Language Model Applications. arXiv:2505.07203 [cs.DC] <https://arxiv.org/abs/2505.07203>
- [9] Jiangfei Duan, Runyu Lu, Haojie Duanmu, Xiuhong Li, Xingcheng Zhang, Dahua Lin, Ion Stoica, and Hao Zhang. 2024. MuxServe: flexible spatial-temporal multiplexing for multiple LLM serving. In *Proceedings of the 41st International Conference on Machine Learning (Vienna, Austria) (ICML '24)*. JMLR.org.
- [10] Jiarui Fang, Jinzhe Pan, Xibo Sun, Aoyu Li, and Jiannan Wang. 2024. xDiT: an Inference Engine for Diffusion Transformers (DiTs) with Massive Parallelism. arXiv:2411.01738 [cs.DC] <https://arxiv.org/abs/2411.01738>
- [11] Flux.1 AI. 2025. *Flux.1 AI Image Generator*. <https://flux1.ai/create>
- [12] Jonathan Ho, Ajay Jain, and Pieter Abbeel. 2020. Denoising diffusion probabilistic models. In *Advances in Neural Information Processing Systems (NeurIPS)*.
- [13] Heyang Huang, Cunchen Hu, Jiaqi Zhu, Ziyuan Gao, Liangliang Xu, Yizhou Shan, Yungang Bao, Sun Ninghui, Tianwei Zhang, and Sa Wang. 2025. DDiT: Dynamic Resource Allocation for Diffusion Transformer Model Serving. arXiv:2506.13497 [cs.DC] <https://arxiv.org/abs/2506.13497>
- [14] Sam Ade Jacobs, Masahiro Tanaka, Chengming Zhang, Minjia Zhang, Shuaiwen Leon Song, Samyam Rajbhandari, and Yuxiong He. 2023. DeepSpeed Ulysses: System Optimizations for Enabling Training of Extreme Long Sequence Transformer Models. arXiv:2309.14509 [cs.LG] <https://arxiv.org/abs/2309.14509>
- [15] Alind Khare, Dhruv Garg, Sukrit Kalra, Snigdha Grandhi, Ion Stoica, and Alexey Tumanov. 2025. SuperServe: Fine-Grained Inference Serving for Unpredictable Workloads. In *22nd USENIX Symposium on Networked Systems Design and Implementation (NSDI 25)*. 739–758.
- [16] Woosuk Kwon, Zhuohan Li, Siyuan Zhuang, Ying Sheng, Lianmin Zheng, Cody Hao Yu, Joseph E. Gonzalez, Hao Zhang, and Ion Stoica. 2023. Efficient Memory Management for Large Language Model Serving with PagedAttention. In *Proceedings of the ACM SIGOPS 29th Symposium on Operating Systems Principles*.
- [17] Black Forest Labs. 2024. *FLUX.1-dev: Text-to-Image Generation Model*.
- [18] Shenggui Li, Fuzhao Xue, Chaitanya Baranwal, Yongbin Li, and Yang You. 2022. Sequence Parallelism: Long Sequence Training from System Perspective. arXiv:2105.13120 [cs.LG] <https://arxiv.org/abs/2105.13120>
- [19] Hao Liu, Matei Zaharia, and Pieter Abbeel. 2023. Ring Attention with Blockwise Transformers for Near-Infinite Context. arXiv:2310.01889 [cs.CL] <https://arxiv.org/abs/2310.01889>
- [20] Yixuan Mei, Yonghao Zhuang, Xupeng Miao, Juncheng Yang, Zhihao Jia, and Rashmi Vinayak. 2025. Helix: Serving Large Language Models over Heterogeneous GPUs and Network via Max-Flow. In *Proceedings of the 30th ACM International Conference on Architectural Support for Programming Languages and Operating Systems (ASPLOS)*. ACM, Rotterdam, Netherlands. doi:10.1145/3669940.3707215
- [21] Xupeng Miao, Gabriele Ollaro, Zhihao Zhang, Xinhao Cheng, Zeyu Wang, Rae Ying Yee Wong, Zhuoming Chen, Daiyaan Arfeen, Reyna Abhyankar, and Zhihao Jia. 2023. SpecInfer: Accelerating Generative LLM Serving with Speculative Inference and Token Tree Verification. *CoRR* abs/2305.09781 (2023). <https://arxiv.org/abs/2305.09781>
- [22] Xupeng Miao, Chunan Shi, Jiangfei Duan, Xiaoli Xi, Dahua Lin, Bin Cui, and Zhihao Jia. 2024. SpotServe: Serving Generative Large Language Models on Preemptible Instances. In *Proceedings of the 29th ACM International Conference on Architectural Support for Programming Languages and Operating Systems (ASPLOS)*, Vol. 2. ACM, 1112–1127.
- [23] NVIDIA. 2022. NVIDIA Collective Communication Library (NCCL) Documentation. <https://docs.nvidia.com/deeplearning/nccl/user-guide/docs/index.html>.
- [24] Christos H Papadimitriou and Kenneth Steiglitz. 1998. *Combinatorial optimization: algorithms and complexity*. Courier Corporation.
- [25] Pratyush Patel, Esha Choukse, Chaojie Zhang, Aashaka Shah, Ñiigo Goiri, Saeed Maleki, and Ricardo Bianchini. 2024. Splitwise: Efficient Generative LLM Inference Using Phase Splitting. In *Proceedings of the International Symposium on Computer Architecture (ISCA)*. ACM, Buenos Aires, Argentina.
- [26] William Peebles and Saining Xie. 2023. Scalable Diffusion Models with Transformers. In *International Conference on Computer Vision (ICCV)*. arXiv:2212.09748 [cs.CV] <https://arxiv.org/abs/2212.09748>

- [27] Olaf Ronneberger, Philipp Fischer, and Thomas Brox. 2015. U-Net: Convolutional networks for biomedical image segmentation. In *International Conference on Medical Image Computing and Computer-Assisted Intervention (MICCAI)*. Springer, 234–241.
- [28] Jascha Sohl-Dickstein, Eric A. Weiss, Niru Maheswaranathan, and Surya Ganguli. 2015. Deep unsupervised learning using nonequilibrium thermodynamics. *arXiv preprint arXiv:1503.03585* (2015).
- [29] Yang Song and Stefano Ermon. 2021. Score-Based Generative Modeling through Stochastic Differential Equations. In *International Conference on Learning Representations (ICLR)*.
- [30] Stability AI. 2024. Stability AI Platform API Reference. <https://platform.stability.ai/docs/api-reference> Accessed: 2024-11-26.
- [31] Ashish Vaswani, Noam Shazeer, Niki Parmar, Jakob Uszkoreit, Llion Jones, Aidan N Gomez, Łukasz Kaiser, and Illia Polosukhin. 2017. Attention is All You Need. In *Advances in Neural Information Processing Systems (NeurIPS)*.
- [32] Zijie J. Wang, Evan Montoya, David Munechika, Haoyang Yang, Benjamin Hoover, and Duen Horng Chau. 2023. DiffusionDB: A Large-scale Prompt Gallery Dataset for Text-to-Image Generative Models. arXiv:2210.14896 [cs.CV] <https://arxiv.org/abs/2210.14896>
- [33] Bingyang Wu, Shengyu Liu, Yinmin Zhong, Peng Sun, Xuanzhe Liu, and Xin Jin. 2024. LoongServe: Efficiently Serving Long-Context Large Language Models with Elastic Sequence Parallelism. arXiv:22405.09526 [cs.DC] <https://arxiv.org/abs/22405.09526>
- [34] Yuchen Xia, Divyam Sharma, Yichao Yuan, Souvik Kundu, and Nishil Talati. 2025. MoDM: Efficient Serving for Image Generation via Mixture-of-Diffusion Models. arXiv:2503.11972 [cs.DC] <https://arxiv.org/abs/2503.11972>
- [35] Hong Zhang, Yupeng Tang, Anurag Khandelwal, and Ion Stoica. 2023. SHEPHERD: Serving DNNs in the wild. In *20th USENIX Symposium on Networked Systems Design and Implementation (NSDI 23)*. 787–808.
- [36] Yanli Zhao, Andrew Gu, Rohan Varma, Liang Luo, Chien-Chin Huang, Min Xu, Less Wright, Hamid Shojanazeri, Myle Ott, Sam Shleifer, et al. 2023. Pytorch fsdp: experiences on scaling fully sharded data parallel. *arXiv preprint arXiv:2304.11277* (2023).
- [37] Lianmin Zheng, Liangsheng Yin, Zhiqiang Xie, Chuyue Sun, Jeff Huang, Cody Hao Yu, Shiyi Cao, Christos Kozyrakis, Ion Stoica, Joseph E. Gonzalez, Clark Barrett, and Ying Sheng. 2024. SGLang: Efficient Execution of Structured Language Model Programs. In *The Thirty-eighth Annual Conference on Neural Information Processing Systems*. <https://openreview.net/forum?id=VqkAKQibpq>